
WaveMix: A Resource-efficient Neural Network for Image Analysis

Pranav Jeevan P¹ Kavitha Viswanathan¹ Anandu A S¹ Amit Sethi¹

Abstract

To allow image analysis in resource-constrained scenarios without compromising generalizability, we introduce WaveMix – a novel and flexible neural framework that reduces the GPU RAM (memory) and compute (latency) compared to CNNs and transformers. In addition to using convolutional layers that exploit shift-invariant image statistics, the proposed framework uses multi-level two-dimensional discrete wavelet transform (2D-DWT) modules to exploit scale-invariance and edge sparseness, which gives it the following advantages. Firstly, the fixed weights of wavelet modules do not add to the parameter count while reorganizing information based on these image priors. Secondly, the wavelet modules scale the spatial extents of feature maps by integral powers of $\frac{1}{2} \times \frac{1}{2}$, which reduces the memory and latency required for forward and backward passes. Finally, a multi-level 2D-DWT leads to a quicker expansion of the receptive field per layer than pooling (which we do not use) and it is a more effective spatial token mixer. WaveMix also generalizes better than other token mixing models, such as ConvMixer, MLP-Mixer, PoolFormer, random filters, and Fourier basis, because the wavelet transform is much better suited for image decomposition and spatial token mixing. WaveMix is a flexible model that can perform well on multiple image tasks without needing architectural modifications. WaveMix achieves a semantic segmentation mIoU of 83% on Cityscapes validation set outperforming transformer and CNN based architectures. We also demonstrate the advantages of WaveMix for classification on multiple datasets and show that WaveMix establishes new state-of-the-results in Places-365, EMNIST and iNAT-mini datasets.

1. Introduction

Ever since it has been demonstrated that convolutional neural networks (CNNs) can achieve generalization for image classification better than dense neural networks (Lecun et al., 1998; Krizhevsky et al., 2012), further improvements have relied on formulating deeper CNNs with architectural and training innovations (Simonyan & Zisserman, 2014; Szegedy et al., 2014; He et al., 2015b; Howard et al., 2017; Hu et al., 2017; Huang et al., 2016). On the other hand, adapting transformers that were developed for natural language processing (NLP) to vision tasks was a departure from exploiting shift-invariance via convolutions, but it highlighted the importance of mixing tokens that are spatially far apart (Zhao et al., 2020; Dosovitskiy et al., 2021). However, forsaking shift-invariance, and adopting global self-attention for token mixing with quadratic complexity meant that the *training and inference requirements have increased to a prohibitive level for most vision applications* (Khan et al., 2022). Linear approximations to quadratic attention reduce the computational requirements only to some extent (Jeevan & Sethi, 2022). Alternative token-mixing architectures have also been proposed to replace self-attention altogether (Tolstikhin et al., 2021; Guibas et al., 2021; Trockman & Kolter, 2022). However, vision transformers and token mixers cannot be easily adapted for multiple image dimensions and vision tasks, such as segmentation (Trockman & Kolter, 2022) without significant architectural changes, nor do they exploit image priors effectively.

While convolutional design elements exploit shift-invariance prior in images, multi-scale self-similarity across spatial scales (eg., due to variable object distance) and sparseness of edges (eg., due to finite spatial extents of objects) are also ubiquitous image priors that have not been explored very well in neural frameworks (with some exceptions (Mei et al., 2020)). The wavelet transform (in its 2D version, where its 1D version is first applied to the rows and then to the columns) captures these priors well and has been widely used in the pre-deep neural network era for various imaging applications, such as compression and denoising (Lewis & Knowles, 1992; Ruikar & Doye, 2010). We propose a neural framework called *WaveMix*, which uses the multi-level two-dimensional discrete wavelet transform (2D-DWT or wavelet transform) as a spatial token mixer that exploits

¹Department of Electrical Engineering, Indian Institute of Technology Bombay, Mumbai, India. Correspondence to: Pranav Jeevan P <194070025@iitb.ac.in>, Amit Sethi <asethi@iitb.ac.in>.

these additional image priors.¹ The contributions of this work are the following:

1. Proposes the first token mixing model that incorporates multi-level 2D-DWT for spatial information mixing as an integral part of each layer block, which exploits scale-invariance and sparseness of edges in images.
2. Utilizes the image-appropriate downsampling properties of wavelets to reduce resource (memory and compute) requirement for channel mixing by the next layer.
3. Devises a fully convolutional framework that does not require significant architectural changes (eg., feature map flattening, up-convolutions, and skip connections (Siam et al., 2018)) to adapt to different image dimensions and tasks. Similar to a transformer encoder, WaveMix preserves the resolution of the feature maps across the blocks, but unlike transformers, it can handle changes in image dimensions well.
4. Demonstrates using Cityscapes dataset that WaveMix networks can meet or exceed semantic segmentation benchmarks with lower GPU RAM consumption and faster processing without being pre-trained using larger datasets.
5. Demonstrates that WaveMix networks can meet or exceed classification accuracy benchmarks with lower GPU RAM consumption and faster forward and backward passes using ImageNet-1k, Places-365, CIFAR, EMNIST, MNIST, Fashion MNIST, SVHN, Tiny ImageNet and iNAT-mini datasets. WaveMix also achieves state-of-the-art (SOTA) results on all five EMNIST datasets, Places-365 and iNAT-mini datasets.
6. Demonstrates that the 2D-DWT is a better token mixer compared to random fixed weights or a 2D Fourier transform (we extended FNet token mixer (Lee-Thorp et al., 2021) to 2D).

After describing how WaveMix is related to previous works in Section 2, we share its design insights and details in Section 3. In Section 4 we compare WaveMix with other models on image classification and semantic segmentation, provide empirical evidence of its scalability, and examine the importance of its components. We conclude and list potential future directions in Section 5.

2. Related Works

Statistical properties of natural images that have been well-studied include shift-invariance (stationarity), scale-

invariance (especially in 2D projections of 3D objects viewed from various distances), high spatial auto-correlation (monochromatic objects or regions), spatial sparseness of edges (finite spatial extent of objects), and preponderance of certain colors (Field, 1993; Ruderman, 1994; Lee, 1996; Párraga et al., 2002). Of these, only the shift-invariance has been widely exploited in neural architectures for image analysis in the form of convolutional architectural elements (Le-Cun et al., 1998; Long et al., 2015). There have been some exceptions that incorporate rotational-invariance for remote sensing images (Cheng et al., 2016) and multi-resolution analysis for segmentation of histopathology images (Kurian et al., 2022; van Rijthoven et al., 2021), but these methods have not been tested on general computer vision benchmarks.

Advances in CNN performance have mainly come from architectural changes with the goals of easing gradient flow to deeper layers (He et al., 2015a; Szegedy et al., 2014), or reducing parameters per layer by restricting convolutional kernel size (Simonyan & Zisserman, 2014) or their scope to only one dimension (Chollet, 2016). Attention mechanisms for space or channel (Chen et al., 2017) also seem to improve performance of CNNs, although it has not been explored why a stack of additional convolutional layers cannot model the same function as that of spatial or channel attention.

Vision transformers and hybrid architectures, inspired by their success on NLP tasks, have pushed the image classification accuracy beyond those of the largest CNNs, albeit at the cost of several times more training data and network parameters (Dosovitskiy et al., 2021). *Training these models with hundreds of millions of parameters requires access to large GPU clusters, which is impractical for resource-constrained applications and scenarios.* Reduction in the computational requirements of vision transformers have been made possible by architectural changes that provide image-specific inductive biases by creating hybrid models with elements including distillation (Touvron et al., 2020), convolutional embeddings (Jeevan & Sethi, 2022; Hassani et al., 2021), convolutional tokens (Wu et al., 2021), and encoding overlapping patches (Yuan et al., 2021). The quadratic complexity with respect to the sequence length (number of pixels) of transformers has also led to the search for other linear approximations of self-attention for efficiently mixing tokens (Jeevan & Sethi, 2022).

Token mixers that replace the self-attention in transformers with fixed token mixing mechanisms, such as the Fourier transform, achieves comparable generalization with lower computational requirements on NLP tasks (Lee-Thorp et al., 2021). Other token-mixing architectures have also been proposed that use standard neural components, such as convolutional layers and multi-layer perceptrons (MLPs) for mixing visual tokens. MLP-mixer uses two MLP layers

¹Our code is available at <https://github.com/pranavphoenix/WaveMix>

(cascade of 1×1 convolutions) applied first to an image patch sequence and then to the channel dimension to mix tokens (Tolstikhin et al., 2021). ConvMixer uses standard convolutions along spatial dimensions and depth-wise convolutions across channels to mix tokens with fewer computations than attention mechanisms (Trockman & Kolter, 2022). These token mixing models perform efficiently compared to transformers without compromising generalization. However, these models do not use image priors well.

Two-dimensional discrete wavelet transform (2D-DWT) has been extensively researched to exploit various multi-resolution properties of images for various applications, including denoising (Ruikar & Doye, 2010), super-resolution (Guo et al., 2017), recognition (Mahmood et al., 2018), and compression (Lewis & Knowles, 1992). Features extracted using wavelet transforms have also been used extensively with machine learning models (Mowlaei et al., 2002), such as support vector machines and neural networks (Ranaware & Deshpande, 2016), especially for image classification (Nayak et al., 2016). Representative instances of integration of wavelets in neural architectures include the following. ScatNet architecture cascades wavelet transform layers with nonlinear modulus and average pooling to extract translation-invariant features that are robust to deformations and preserve high-frequency information for image classification (Bruna & Mallat, 2013). WaveCNets replaces max-pooling, strided-convolution, and average-pooling of CNNs with 2D-DWT for noise-robust image classification (Li et al., 2020a). Multi-level wavelet CNN (MWCNN) has been used for image restoration as well as with UNet architectures for better trade-off between receptive field size and computational efficiency (Liu et al., 2018). Wavelet transform has also been combined with a fully convolutional neural network for image super-resolution (Kumar et al., 2017). Pooling using wavelets have been shown to perform comparably with other pooling techniques (Williams & Li, 2018). WaveSNet uses DWT to downsample and inverse-DWT to upsample feature maps in UNets for segmentation (Li & Shen, 2020)

3. WaveMix Architectural Framework

Image pixels have several interesting co-dependencies. The localized and stationary nature of image patch statistics have been exploited using space-invariant filters (convolutional kernels) of limited size. However, we think that scale-invariance and edge localization can be better modeled by wavelet decomposition due to its natural properties that are well-suited for multi-resolution analysis. When combined with learnable convolutional filters, the proposed framework may more comprehensively exploit space-invariance as well.

3.1. Overall architecture

As shown in Figure 1 (a) and (b), the macro-level idea behind the proposed framework is to stack WaveMix blocks that, by design, are fully convolutional in both spatial dimensions *and* maintain the spatial resolution of the feature maps across the blocks. While some CNNs are fully convolutional, vision transformer architectures tend to maintain the sequence lengths (which is a flattened version of the spatial resolution). Combining these two elements gives WaveMix architectural flexibility to easily adapt to various image dimensions and tasks. For instance, while pixel maps for semantic segmentation or image enhancement are a natural outcome of this framework, adding global average pooling and softmax layers are enough to adapt it for classification of images of various sizes. That is, WaveMix processes image as a 2D grid and not as sequence of pixels/patches by unrolling the image as done in transformer models. Additionally, it does not collapse the spatial resolution of the feature maps, unlike a CNN.

An initial convolutional layer is used (Figure 1 (a) and (b)) to increase the number of channels before passing it to WaveMix blocks. It can also be used optionally to reduce the input resolution either using strided convolutions or patchifying convolutions (Trockman & Kolter, 2022; Liu et al., 2022). After the stack of WaveMix blocks, an MLP layer can be used to mix channels for image classification (Figure 1 (a)), or a transposed convolutional layer can be used to expand resolution for semantic segmentation or image restoration (Figure 1 (b)). Appropriate task-specific layers can then attached to the end, such as a global average pooling (to process images of various sizes) and a softmax layer for classification, or a per-pixel softmax layer for semantic segmentation (Figure 1 (a) and (b)).

3.2. WaveMix block

As shown in Figure 1 (c), the micro-level idea behind our proposed framework is extracting learnable and space-invariant features using a convolutional layer, followed by spatial token-mixing and downsampling for scale-invariant feature extraction using 2D-DWT², followed by channel-mixing using a learnable MLP (1×1 conv) layer, followed by restoring spatial resolution of the feature map using a transposed-convolutional layer.

The use of trainable convolutions *before* the wavelet transform is a key design aspect of our architecture as it allows the extraction of only those feature maps that are suitable for the chosen wavelet basis functions. The convolutional layer decreases the embedding dimension (number of channels C , a hyper-parameter) by a factor of four so that the con-

²Base wavelet code: <https://pytorch-wavelets.readthedocs.io/en/latest/readme.html>

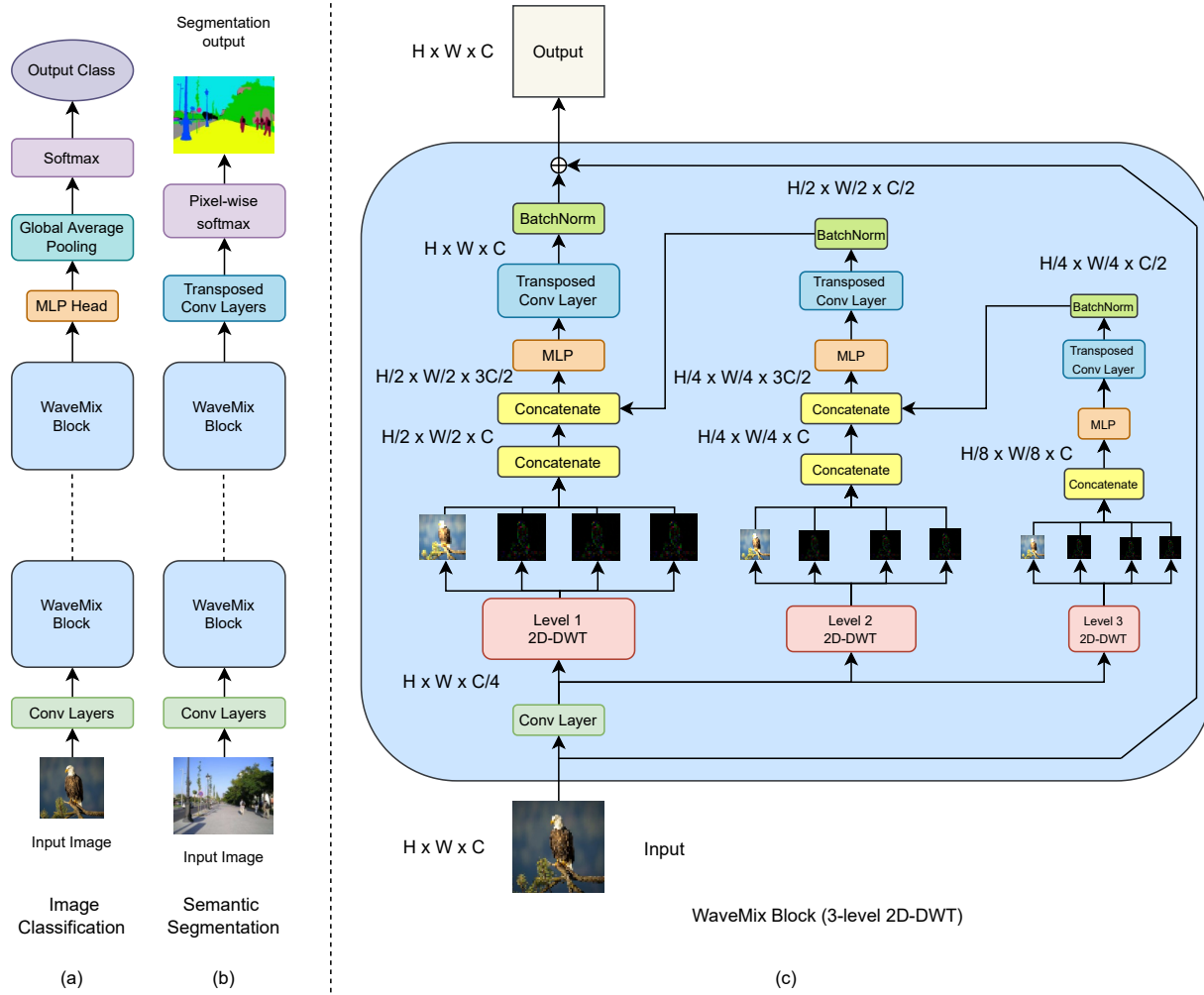


Figure 1. WaveMix architecture for (a) image classification and (b) semantic segmentation, along with (c) details of the WaveMix block

concatenated output after the Level-1 2D-DWT has the same number of channels as the input. That is, since 2D-DWT is a lossless transform, it expands the number of channels by the same factor (using concatenation) by which it reduces the spatial resolution by computing an approximation sub-band (low-resolution approximation) and three detail sub-bands (spatial derivatives) (Daubechies, 1990) for each input channel. This combination requires fewer layers and parameters than using only convolutional layers with pooling, which we do not use. The lossless property of 2D-DWT leads to accuracy gains over using pooling while still reducing the number of computations for the subsequent MLP layer due to the down-sampling.

The number of levels of wavelet decomposition used is decided based on the image size. Each level reduces the output size by a factor of 2×2 . Our experiments show that using three or four levels of 2D-DWT are sufficient to ensure

token-mixing over long spatial distances. For instance, a 3-level DWT decomposition of an image of size 64×64 simultaneously creates feature maps of size 32×32 , 16×16 , and 8×8 , which are sufficient for spatial token mixing by the transposed-convolution layer. Using more levels of DWT increases the receptive field exponentially, but it also amplifies noise in the model (Daubechies, 1990), which degrades the performance. The number of channels of a higher level DWT are reduced using an MLP layer and the spatial resolution of its feature maps is expanded using transposed convolutional layer before using batch norm and concatenating the output with the feature maps of the previous level.

The concatenated output of the wavelet layer is passed to an MLP layer, which has two 1×1 convolutional layers with an inverse bottleneck design (multiplication factor > 1) separated by a GELU non-linearity. After this, the feature map resolution is expanded to match that of the block’s input

using transposed-convolutions (up-convolutions) followed by batch normalization, and a residual connection is used to ease the flow of the gradient (He et al., 2015a). We do not use up-convolution in each branch to directly resize image back to the original input resolution because doing so will require large-sized filters, which will lead to parameter expansion.

The lower levels of the DWT capture the finer details of the image while higher levels capture more global information (Bruna & Mallat, 2013). The feed-forward (MLP) sub-layers immediately following DWT have access to the outputs at the corresponding level and those from higher levels (after transposed-convolution) to learn both local and global features. As the information from higher levels propagate to lower levels, mixing of local and global information enables the model to learn efficiently with fewer parameters and layers.

Among the different types of mother wavelets available, we used the Haar wavelet (a special case of the Daubechies wavelet (Daubechies, 1990), also known as Db1), which is frequently used due to its simplicity and faster computation. Haar wavelet is both orthogonal and symmetric in nature, and has been extensively used to extract basic structural information from images (Porwik & Lisowska, 2004). For even-sized images, it reduces the dimensions exactly by a factor of 2, which simplifies the designing of the subsequent layers.

4. Experiments and Results

4.1. Tasks, datasets, and models compared

WaveMix models were compared with various CNN, transformer, and token-mixing models for semantic segmentation and image classification.

For semantic segmentation, we used the Cityscapes (Cordts et al., 2016) dataset (under MIT Licenses). The official training dataset itself was split into training and validation sets. Results of the other models compared were directly taken from their original papers as cited in Table 1. Since ConvMixer (Trockman & Kolter, 2022) was never used for semantic segmentation, the classification head of ConvMixer was replaced with a segmentation head similar to WaveMix for segmentation experiments. Mean intersection over union (mIoU) on the Cityscapes official validation dataset was compared as a generalization metric among the models. Inference throughput on a single GPU was reported in frames/sec (FPS).

For classification, we used multiple types of publicly available (under MIT Licenses) datasets based on the number of images and image size. Small datasets (with 100,000 training images or fewer) of smaller image sizes (64×64

or smaller) included CIFAR-10, CIFAR-100 (Krizhevsky, 2009), EMNIST (Cohen et al., 2017), Fashion MNIST (Xiao et al., 2017), SVHN (Netzer et al., 2011) and Tiny ImageNet (Le & Yang, 2015). We also used larger datasets with larger images sizes, such as ImageNet-1K (Deng et al., 2009), Places-365 (Zhou et al., 2017), and iNaturalist2021-10k (iNAT-2021-mini) (Horn et al., 2021). The models compared for image classification on ImageNet-1k dataset include ResNets (He et al., 2015a) and MobileNetV3 (Howard et al., 2019) as CNNs; ViT (vision transformer) (Dosovitskiy et al., 2021), LeViT (Graham et al., 2021) and PiT (Pooling-based vision transformer) (Heo et al., 2021) as transformers; and ConvMixer (Trockman & Kolter, 2022), MLP-Mixer (Tolstikhin et al., 2021) and PoolFormer (Yu et al., 2021) as token-mixers. Other models used are MobileNet (Sandler et al., 2018), hybrid ViN (vision Nystrom-former) (Jeevan & Sethi, 2022), CPV (convolutional performer for vision) (Jeevan & sethi, 2022), CCT (compact convolutional transformer) (Hassani et al., 2021), CvT (convolutional vision transformer) (Wu et al., 2021), and our 2D extension of FNet (Lee-Thorp et al., 2021). Top-1 accuracy on the test set of the best of three runs with random initialization is reported as a generalization metric based on prevailing protocols (Hassani et al., 2021). For Places-365 and iNAT-mini datasets, we have reported Top-1 accuracy in validation set. GPU RAM usage for a fixed batch size of 64 is reported in the appendix.

For model notation, we use the format *Model Name-Embedding Dimension/Layers*×*Heads* for transformers and exclude the *heads* for the other architectures. For example, CPV with embedding dimension of 128 having 4 layers and 4 heads is labelled as CPV-128/4×4. We call the WaveMix model which uses only one level of 2D-DWT as *WaveMix-Lite* and it has been shown to perform well in small datasets with low resolution images. For other models, we use the same notation that is used in their original papers.

4.2. Implementation details

We adjusted the stride (or patch size) in the initial convolutional layers in all WaveMix models that handled high-resolution images to ensure that smaller side of input before it reached WaveMix blocks was always less than 64 for classification and 256 for segmentation. We only used strided convolutions in the initial convolution layers for segmentation, and classification of datasets with smaller image sizes (less than 128×128). For classification of datasets with *No pre-training was performed on any of the WaveMix models unless specified*. For classification on ImageNet-1K, we used the models available in Timm (PyTorch Image Models) library (Wightman, 2019) without using pre-trained weights and used the Timm training script with default hyper-parameter values.

Table 1. Results for semantic segmentation on Cityscapes validation set show improved mIoU by WaveMix without compromising inference throughput (FPS)

ARCHITECTURE	mIoU \uparrow	# PARAM. \downarrow	FPS \uparrow	NOTES
UNET (SIAM ET AL., 2018)	57.90	28.9 M	1	RESNET-18 ENCODER
UNET (SIAM ET AL., 2018)	61.00	9.0 M	-	MOBILENETV2 ENCODER
DEEPLABV3+ (CHEN ET AL., 2018)	80.90	62.7 M	1	RESNET-101 ENCODER
AXIAL-DEEPLAB (WANG ET AL., 2020A)	81.10	-	-	AXIALRESNET-XL ENCODER
SEGFORMER (XIE ET AL., 2021)	82.30	64.1 M	3	MIT-B4 ENCODER
SEG-L-MASK/16 (STRUDEL ET AL., 2021)	81.30	307 M	-	VIT-L BACKBONE
CONVMIXER-256/14	70.90	1.7 M	9	NO PRETRAINING
WAVEMIX-256/16 (4 LEVEL)	78.64	63.2 M	7	NO PRETRAINING
WAVEMIX-256/16 (4 LEVEL)	82.60	63.2 M	7	IMAGENET PRETRAINED

Due to limited computational resources (which actually inspired looking for an alternative neural framework), the *maximum number of training epochs was set to 300*. All experiments were done with a single 80 GB Nvidia A100 GPU. For all experiments other than training ImageNet-1k, we used AdamW optimizer ($\alpha = 0.001, \beta_1 = 0.9, \beta_2 = 0.999, \epsilon = 10^{-8}$) with a weight decay coefficient of 0.01 during initial epochs and then used SGD (stochastic gradient descent) with learning rate of 0.001 and momentum = 0.9 during the final 50 epochs (Keskar & Socher, 2017; Jeevan & sethi, 2022). Cross-entropy loss was used for image classification and pixel-wise focal loss was used for semantic segmentation. A batch-size of 5 was used for all segmentation experiments with full resolution cityscapes dataset. Batch-size between 256-512 was used in most of the classification tasks. We used the largest ConvMixer model that could fit in a single GPU. We used automatic mixed precision in PyTorch during training to optimize speed and memory consumption.

4.3. Semantic segmentation

WaveMix can be directly used for semantic segmentation by replacing the classifier head with two deconvolution layers and a per-pixel softmax layer to generate the segmentation maps. On the other hand, architectural changes – such as encoder-decoder and skip connections (Ronneberger et al., 2015) – are required for base CNNs and transformers, including SegFormer (Xie et al., 2021), to perform segmentation.

Performance of WaveMix on Cityscapes validation set along with the reported results of other models are shown in Table 1. We used the full resolution input of 1024×2048 for training WaveMix. Even without ImageNet pre-training, WaveMix performs on par with the other models which uses encoders pre-trained on ImageNet. After using ImageNet pre-trained weights, WaveMix outperforms all the other CNN and transformer-based models. WaveMix is also faster than the other models in inference throughput even on a

single GPU. It outperforms current state-of-the-art models like SegFormer (Xie et al., 2021) in terms of mIoU and throughput.

The lower mIoU obtained by replacing the classification head of ConvMixer (Trockman & Kolter, 2022) with segmentation head (similar to WaveMix) shows that token-mixing architectures, which work well for classification, does not translate that performance to segmentation tasks without significant architectural modifications. This shows the versatility of our model. Also, the GPU consumption of WaveMix is much lower than ConvMixer even though WaveMix has higher parameter count. The parametric efficiency of ConvMixer is overshadowed by its large GPU requirements. See appendix materials for details.

4.4. Image classification

Table 2 shows the performance of WaveMix on image classification using supervised learning on ImageNet-1K on a single GPU with limited epochs. WaveMix models outperform CNN and transformer-based models, and token-mixers like ConvMixer, MLP-Mixer and PoolFormer. Even though convolution has been widely regarded as a GPU-efficient operation, the need for deeper architectures have necessitated the use of networks having over a hundred layers for achieving strong generalization. Even though a single convolutional operation is comparatively cheaper than a 2D-DWT, we can achieve generalization comparable to deep convolutional networks with far fewer layers of WaveMix. This ability of the wavelet transform to provide competitive performance without needing large number of layers helps in improving the efficiency of the network by consuming much lesser GPU RAM than deep convolutional models such as ResNets. The use of non-learnable fixed weights and shallower network structure also makes inference using WaveMix faster than other architectures. Details on inference speed and GPU consumption is provided in the appendix.

Table 3 and Table 4 shows the performance of WaveMix for

Table 2. Results of Image classification on ImageNet-1K dataset (224×224) using Timm training script (Wightman, 2019) on a single GPU shows improved accuracy as well as decreased parameter count by WaveMix.

MODELS	#PARAMS (M)	TOP-1 ACC. (%)
RESNET-18	11.7	69.06
RESNET-34	21.8	72.27
RESNET-50	25.6	73.61
MOBILENETV3-LARGE 0.75	4.0	69.84
VIT-TINY-PATCH-16	5.7	67.72
VIT-SMALL-PATCH-16	22.0	67.81
VIT-BASE-PATCH-16	86.6	66.93
LEVIT-128	9.2	68.03
LEVIT-256	18.9	70.44
PIT-SMALL	23.5	71.67
PIT-BASE	73.8	73.58
MLP-MIXER-SMALL-PATCH-16	18.5	60.13
MLP-MIXER-BASE-PATCH-16	59.9	59.84
POOLFORMER-SMALL-12	11.9	54.21
WAVEMIX-128/8 (LEVEL 3)	7.3	62.14
WAVEMIX-192/16 (LEVEL 3)	28.9	74.93

Table 3. Results of WaveMix image classification on various datasets with varying image sizes when trained on a single GPU. See appendix for architectural details and comparison with ResNets.

DATASETS	WAVEMIX TOP-1 ACCU. (%)
MNIST	99.75
FASHION MNIST	94.32
CIFAR-10	97.29
CIFAR-100	85.09
SVHN	98.73
TINYIMAGENET	77.47

image classification on multiple datasets with image sizes ranging from small to large. WaveMix achieved state-of-the-art (SOTA) accuracy of 56.45% on Places-365 standard validation set (224×224) among the models that were not pre-trained on larger datasets, such as (Wang et al., 2020b). It has also achieved SOTA accuracy on iNAT-2021-mini validation set (224×224). We also see from Table 4 that WaveMix models establishes a new state-of-the-art on the smaller EMNIST datasets (28×28) by outperforming the previous best results (Kabir et al., 2020; Pad et al., 2020) for Balanced, Letters, Digits, Byclass and Bymerge subsets within EMNIST (Cohen et al., 2017) without using data augmentations.

4.5. Parameter efficiency

Since WaveMix heavily uses kernels with fixed weights for token mixing, it uses far fewer parameters compared to

Table 4. WaveMix outperforms all previous models for image classification and achieves State-of-the-Art (SOTA) results on all five EMNIST datasets, Places-365 validation set (365 classes) and INAT-mini validation set (10,000 classes). See supplementary materials for architectural details.

DATASETS	SOTA TOP-1 ACCU. (%)
EMNIST BYCLASS	88.43
EMNIST BYMERGE	91.80
EMNIST LETTERS	95.96
EMNIST DIGITS	99.82
EMNIST BALANCED	91.06
PLACES-365 (VALIDATION SET)	56.45
INAT-MINI (VALIDATION SET)	61.75

commonly used architectures. Table 5 shows that WaveMix meets certain accuracy benchmarks with far fewer parameters compared to previous models (Jha et al., 2021; Wu, 2018). We can further reduce the parameter count of WaveMix by replacing the deconvolution layers with upsampling layers using predetermined interpolation techniques (eg., inverse-DWT, bilinear or bicubic).

4.6. Ablation studies

We performed ablation studies using ImageNet-1k and CIFAR-10 datasets on WaveMix to understand the effect of each type of layer on performance by removing the 2D-DWT layer, replacing it with Fourier transform or random filters, as well as learnable wavelets. All of these led to a decrease in accuracy. Those methods that did not reduce the feature map resolution also led to an increase in GPU RAM consumption.

When we removed the 2D-DWT layers from WaveMix, the GPU RAM requirement of the model increased by 62 % and accuracy fell by 5%. This is due to the MLP receiving the full resolution instead of the half-resolution feature map from 2D-DWT.

Replacing the 2D-DWT with the real part of a 2D-discrete Fourier transform (2D-DFT) showed 12% decrease in accuracy along with 73% increase in GPU consumption as the Fourier transform does not downscale a feature map. Additionally, unlike the wavelet transform, the Fourier transform has spatially smoothly (as opposed to abruptly) varying kernels with global (as opposed to local or compact) scope, which do not model object edges due to finite spatial extents in a sparse manner.

Replacing the filters of 2D-DWT with random filters of similar size as Haar wavelet resulted in 6% fall in accuracy, confirming that the fixed kernel weights of 2D-DWT is already well-suited for image analysis based on previous studies.

Table 5. WaveMix needs very few parameters to achieve certain benchmark results compared to other architectures

TASK	MODEL	PARAMETERS	EXPANSION
99% ACCURACY ON MNIST	WAVEMIX-LITE-8/10	3,566	UPSAMPLING
90% ACCURACY ON FASHION MNIST	WAVEMIX-LITE-8/5	7,156	DECONVOLUTION
80% ACCURACY ON CIFAR-10	WAVEMIX-LITE-32/7	37,058	UPSAMPLING
90% ACCURACY ON CIFAR-10	WAVEMIX-LITE-64/6	520,106	DECONVOLUTION

GPU RAM consumption increased by 8% and accuracy decreased by 5% when we replaced the 2D-DWT with 2×2 max pooling, indicating that the loss of information by the latter hurts generalization.

We used lifting scheme (Bastidas Rodriguez et al., 2020) to create learnable wavelet coefficients and observed a decline in performance compared to fixed Haar wavelet coefficients. We also experimented with different wavelet coefficients, such as Daubechies, Coiflet, and Symlet series and observed that Haar wavelet was faster and gave more accurate test results than the others. We think that although higher order Daubechies and the other wavelets are perhaps better suited for information compression of natural images, the feature maps after the first convolutional layer are already sparse and are perhaps better analyzed by the Haar wavelet itself.

We compared upsampling by deconvolution in WaveMix block by replacing it with inverse-2D-DWT and bi-linear upsampling layers. Both inverse 2D-DWT and bi-linear upsampling layers needed more WaveMix blocks compared to deconvolutions to give similar performance. Even though the number of parameters was lower than deconvolution, the larger depth led to consumption of more GPU RAM and slower training and inference.

Additional details of ablation studies on the number of layers, levels of DWT, embedding dimension, MLP dimension, different types of wavelets other than Haar, and learnable wavelets are included in the appendix.

5. Conclusions, Future Directions, and Impact

We proposed a novel and versatile neural architectural framework – WaveMix – that can generalize at par with both CNNs and vision transformers, and their hybrids for image classification and segmentation, while needing fewer parameters, GPU RAM, and clock time. In addition to convolutions, WaveMix uses multi-resolution 2D wavelet transform for token-mixing in images, which exploits additional image priors, such as scale-invariance and finite spatial extents of objects. Unlike CNNs, WaveMix mixes tokens from far apart as it quickly expands the receptive field by reducing the spatial resolution of feature maps through multi-level wavelet transform. And, unlike transformers that unroll a 2D image into a 1D sequence, which makes them rigidly wedded to an image size or proportions, WaveMix

handles the image in its 2D format itself. It is easy to adapt WaveMix for different image sizes and tasks, such as image classification and semantic segmentation, without changing its core architecture, as shown by our experiments on multiple datasets and tasks. WaveMix establishes new SOTA accuracy levels on a few benchmark image datasets.

Although our own lack of computational resources inspired the search for an alternative neural framework, and WaveMix generalized well within the constraints of limited epochs and single GPU on large data sets, its absolute limit of accuracy on large datasets without these constraints needs to be tested (e.g., on hyper-parameter-tuned Timm training script (Wightman, 2019)). Additionally, WaveMix should also be tested on other vision tasks, such as object detection and image enhancement (eg., super-resolution, deblurring, denoising, and inpainting) using task-specific architectural variations. Optimizing the wavelet implementation can further accelerate training and inference of WaveMix Models. One may experiment with the use of different wavelet bases for different stages of WaveMix blocks. Additional image priors can also be exploited in search for resource-efficient neural frameworks for images and videos, such as rotational-invariance.

The high accuracy of image classification by transformers and CNNs comes with high costs in terms of training data, computations, GPU RAM, hardware costs, form factors, and energy consumption (Li et al., 2020b). Our research shows that architectural innovations can still reduce these computational requirements by exploiting priors of natural images, such as scale-invariance and finite spatial extents (in addition to shift-invariance that is already exploited by convolutional design elements), without sacrificing accuracy. Such architectures would also be more environment-friendly due to lower energy consumption and accessible for modification to more researchers and deployment scenarios where compute resources are finite. Additionally, we hope that this work inspires others to think of ways to exploit other image and video priors while designing neural frameworks for computer vision.

References

Bastidas Rodriguez, M. X., Gruson, A., Polanía, L. F., F ujieda, S., Ortiz, F. P., Takayama, K., and Hachisuka, T.

- Deep adaptive wavelet network. In *2020 IEEE Winter Conference on Applications of Computer Vision (WACV)*, pp. 3100–3108, 2020. doi: 10.1109/WACV45572.2020.9093580.
- Bruna, J. and Mallat, S. Invariant scattering convolution networks. *IEEE Transactions on Pattern Analysis and Machine Intelligence*, 35(8):1872–1886, 2013. doi: 10.1109/TPAMI.2012.230.
- Chen, L., Zhang, H., Xiao, J., Nie, L., Shao, J., Liu, W., and Chua, T.-S. Sca-cnn: Spatial and channel-wise attention in convolutional networks for image captioning. In *Proceedings of the IEEE Conference on Computer Vision and Pattern Recognition (CVPR)*, July 2017.
- Chen, L.-C., Zhu, Y., Papandreou, G., Schroff, F., and Adam, H. Encoder-decoder with atrous separable convolution for semantic image segmentation, 2018. URL <https://arxiv.org/abs/1802.02611>.
- Cheng, G., Zhou, P., and Han, J. Learning rotation-invariant convolutional neural networks for object detection in vhr optical remote sensing images. *IEEE Transactions on Geoscience and Remote Sensing*, 54(12):7405–7415, 2016.
- Chollet, F. Xception: Deep learning with depthwise separable convolutions, 2016. URL <https://arxiv.org/abs/1610.02357>.
- Cohen, G., Afshar, S., Tapson, J., and van Schaik, A. Emnist: Extending mnist to handwritten letters. In *2017 International Joint Conference on Neural Networks (IJCNN)*, pp. 2921–2926, 2017. doi: 10.1109/IJCNN.2017.7966217.
- Cordts, M., Omran, M., Ramos, S., Rehfeld, T., Enzweiler, M., Benenson, R., Franke, U., Roth, S., and Schiele, B. The cityscapes dataset for semantic urban scene understanding, 2016. URL <https://arxiv.org/abs/1604.01685>.
- Cubuk, E. D., Zoph, B., Shlens, J., and Le, Q. V. Randaugment: Practical automated data augmentation with a reduced search space, 2019.
- Daubechies, I. The wavelet transform, time-frequency localization and signal analysis. *IEEE Transactions on Information Theory*, 36(5):961–1005, 1990. doi: 10.1109/18.57199.
- Deng, J., Dong, W., Socher, R., Li, L.-J., Li, K., and Fei-Fei, L. Imagenet: A large-scale hierarchical image database. In *2009 IEEE Conference on Computer Vision and Pattern Recognition*, pp. 248–255, 2009. doi: 10.1109/CVPR.2009.5206848.
- Dosovitskiy, A., Beyer, L., Kolesnikov, A., Weissenborn, D., Zhai, X., Unterthiner, T., Dehghani, M., Minderer, M., Heigold, G., Gelly, S., Uszkoreit, J., and Houslsby, N. An image is worth 16x16 words: Transformers for image recognition at scale, 2021.
- Field, D. Scale-invariance and self-similar ‘wavelet’ transforms: an analysis of natural scenes and mammalian visual systems. *Wavelets, fractals, and Fourier transforms*, pp. 151–193, 1993.
- Gotmare, A. D., Keskar, N. S., Xiong, C., and Socher, R. A closer look at deep learning heuristics: Learning rate restarts, warmup and distillation. *ArXiv*, abs/1810.13243, 2019.
- Graham, B., El-Nouby, A., Touvron, H., Stock, P., Joulin, A., Jégou, H., and Douze, M. Levit: a vision transformer in convnet’s clothing for faster inference, 2021. URL <https://arxiv.org/abs/2104.01136>.
- Guibas, J., Mardani, M., Li, Z., Tao, A., Anandkumar, A., and Catanzaro, B. Adaptive fourier neural operators: Efficient token mixers for transformers, 2021. URL <https://arxiv.org/abs/2111.13587>.
- Guo, T., Mousavi, H. S., Vu, T. H., and Monga, V. Deep wavelet prediction for image super-resolution. In *2017 IEEE Conference on Computer Vision and Pattern Recognition Workshops (CVPRW)*, pp. 1100–1109, 2017. doi: 10.1109/CVPRW.2017.148.
- Hassani, A., Walton, S., Shah, N., Abuduweili, A., Li, J., and Shi, H. Escaping the big data paradigm with compact transformers, 2021.
- He, K., Zhang, X., Ren, S., and Sun, J. Deep residual learning for image recognition, 2015a.
- He, K., Zhang, X., Ren, S., and Sun, J. Deep residual learning for image recognition, 2015b. URL <https://arxiv.org/abs/1512.03385>.
- Heo, B., Yun, S., Han, D., Chun, S., Choe, J., and Oh, S. J. Rethinking spatial dimensions of vision transformers, 2021. URL <https://arxiv.org/abs/2103.16302>.
- Horn, G. V., Cole, E., Beery, S., Wilber, K., Belongie, S., and Aodha, O. M. Benchmarking representation learning for natural world image collections, 2021.
- Howard, A., Sandler, M., Chu, G., Chen, L.-C., Chen, B., Tan, M., Wang, W., Zhu, Y., Pang, R., Vasudevan, V., Le, Q. V., and Adam, H. Searching for mobilenetv3, 2019. URL <https://arxiv.org/abs/1905.02244>.

- Howard, A. G., Zhu, M., Chen, B., Kalenichenko, D., Wang, W., Weyand, T., Andreetto, M., and Adam, H. Mobilenets: Efficient convolutional neural networks for mobile vision applications, 2017. URL <https://arxiv.org/abs/1704.04861>.
- Hu, J., Shen, L., Albanie, S., Sun, G., and Wu, E. Squeeze-and-excitation networks, 2017. URL <https://arxiv.org/abs/1709.01507>.
- Huang, G., Liu, Z., van der Maaten, L., and Weinberger, K. Q. Densely connected convolutional networks, 2016. URL <https://arxiv.org/abs/1608.06993>.
- Jeevan, P. and Sethi, A. Resource-efficient hybrid x-formers for vision. In *Proceedings of the IEEE/CVF Winter Conference on Applications of Computer Vision (WACV)*, pp. 2982–2990, January 2022.
- Jeevan, P. and sethi, A. Convolutional xformers for vision, 2022. URL <https://arxiv.org/abs/2201.10271>.
- Jha, D., Yazidi, A., Riegler, M. A., Johansen, D., Johansen, H. D., and Halvorsen, P. Lightlayers: Parameter efficient dense and convolutional layers for image classification, 2021. URL <https://arxiv.org/abs/2101.02268>.
- Kabir, H. M. D., Abdar, M., Jalali, S. M. J., Khosravi, A., Atiya, A. F., Nahavandi, S., and Srinivasan, D. Spinalnet: Deep neural network with gradual input. *ArXiv*, abs/2007.03347, 2020.
- Keskar, N. S. and Socher, R. Improving generalization performance by switching from adam to sgd, 2017.
- Khan, S., Naseer, M., Hayat, M., Zamir, S. W., Khan, F. S., and Shah, M. Transformers in vision: A survey. *ACM Computing Surveys*, jan 2022. doi: 10.1145/3505244. URL <https://doi.org/10.1145%2F3505244>.
- Krizhevsky, A. Learning multiple layers of features from tiny images. Technical report, 2009.
- Krizhevsky, A., Sutskever, I., and Hinton, G. E. Imagenet classification with deep convolutional neural networks. *Advances in neural information processing systems*, 25, 2012.
- Kumar, N., Verma, R., and Sethi, A. Convolutional neural networks for wavelet domain super resolution. *Pattern Recognition Letters*, 90:65–71, 2017.
- Kurian, N. C., Lohan, A., Verghese, G., Dharamshi, N., Meena, S., Li, M., Liu, F., Gillet, C., Rane, S., Grigoriadis, A., and Sethi, A. Deep multi-scale u-net architecture and noise-robust training strategies for histopathological image segmentation, 2022. URL <https://arxiv.org/abs/2205.01777>.
- Langley, P. Crafting papers on machine learning. In Langley, P. (ed.), *Proceedings of the 17th International Conference on Machine Learning (ICML 2000)*, pp. 1207–1216, Stanford, CA, 2000. Morgan Kaufmann.
- Le, Y. and Yang, X. Tiny imagenet visual recognition challenge, 2015.
- Lecun, Y., Bottou, L., Bengio, Y., and Haffner, P. Gradient-based learning applied to document recognition. *Proceedings of the IEEE*, 86(11):2278–2324, 1998. doi: 10.1109/5.726791.
- LeCun, Y., Bottou, L., Bengio, Y., and Haffner, P. Gradient-based learning applied to document recognition. In *Proceedings of the IEEE*, volume 86, pp. 2278–2324, 1998. URL <http://citeseerx.ist.psu.edu/viewdoc/summary?doi=10.1.1.42.7665>.
- Lee, T. S. Image representation using 2d gabor wavelets. *IEEE Transactions on pattern analysis and machine intelligence*, 18(10):959–971, 1996.
- Lee-Thorp, J., Ainslie, J., Eckstein, I., and Ontanon, S. Fnet: Mixing tokens with fourier transforms, 2021.
- Lewis, A. and Knowles, G. Image compression using the 2-d wavelet transform. *IEEE Transactions on Image Processing*, 1(2):244–250, 1992. doi: 10.1109/83.136601.
- Li, Q. and Shen, L. Wavesnet: Wavelet integrated deep networks for image segmentation, 2020. URL <https://arxiv.org/abs/2005.14461>.
- Li, Q., Shen, L., Guo, S., and Lai, Z. Wavelet integrated cnns for noise-robust image classification, 2020a.
- Li, Z., Wallace, E., Shen, S., Lin, K., Keutzer, K., Klein, D., and Gonzalez, J. Train big, then compress: Rethinking model size for efficient training and inference of transformers. In *International Conference on Machine Learning*, pp. 5958–5968. PMLR, 2020b.
- Liu, P., Zhang, H., Zhang, K., Lin, L., and Zuo, W. Multi-level wavelet-cnn for image restoration, 2018.
- Liu, Z., Mao, H., Wu, C.-Y., Feichtenhofer, C., Darrell, T., and Xie, S. A convnet for the 2020s, 2022. URL <https://arxiv.org/abs/2201.03545>.
- Long, J., Shelhamer, E., and Darrell, T. Fully convolutional networks for semantic segmentation. In *Proceedings of the IEEE conference on computer vision and pattern recognition*, pp. 3431–3440, 2015.

- Mahmood, M., Jalal, A., and Evans, H. A. Facial expression recognition in image sequences using 1d transform and gabor wavelet transform. In *2018 International Conference on Applied and Engineering Mathematics (ICAEM)*, pp. 1–6, 2018. doi: 10.1109/ICAEM.2018.8536280.
- Mei, Y., Fan, Y., Zhang, Y., Yu, J., Zhou, Y., Liu, D., Fu, Y., Huang, T. S., and Shi, H. Pyramid attention networks for image restoration, 2020. URL <https://arxiv.org/abs/2004.13824>.
- Mowlaei, A., Faez, K., and Haghghat, A. Feature extraction with wavelet transform for recognition of isolated handwritten farsi/arabic characters and numerals. In *2002 14th International Conference on Digital Signal Processing Proceedings. DSP 2002 (Cat. No.02TH8628)*, volume 2, pp. 923–926 vol.2, 2002. doi: 10.1109/ICDSP.2002.1028240.
- Nayak, D. R., Dash, R., and Majhi, B. Brain mr image classification using two-dimensional discrete wavelet transform and adaboost with random forests. *Neurocomputing*, 177: 188–197, 2016.
- Netzer, Y., Wang, T., Coates, A., Bissacco, A., Wu, B., and Ng, A. Y. Reading digits in natural images with unsupervised feature learning, 2011.
- Pad, P., Narduzzi, S., Kundig, C., Turetken, E., Bigdeli, S. A., and Dunbar, L. A. Efficient neural vision systems based on convolutional image acquisition. In *Proceedings of the IEEE/CVF Conference on Computer Vision and Pattern Recognition (CVPR)*, June 2020.
- Párraga, C., Troscianko, T., and Tolhurst, D. Spatiochromatic properties of natural images and human vision. *Current biology*, 12(6):483–487, 2002.
- Porwik, P. and Lisowska, A. The haar-wavelet transform in digital image processing: Its status and achievements. *Machine graphics & vision*, 13:79–98, 2004.
- Ranaware, P. N. and Deshpande, R. A. Detection of arrhythmia based on discrete wavelet transform using artificial neural network and support vector machine. In *2016 International Conference on Communication and Signal Processing (ICCSP)*, pp. 1767–1770, 2016. doi: 10.1109/ICCSP.2016.7754470.
- Ronneberger, O., Fischer, P., and Brox, T. U-net: Convolutional networks for biomedical image segmentation, 2015. URL <https://arxiv.org/abs/1505.04597>.
- Ruderman, D. L. The statistics of natural images. *Network: computation in neural systems*, 5(4):517, 1994.
- Ruikar, S. and Doye, D. D. Image denoising using wavelet transform. In *2010 International Conference on Mechanical and Electrical Technology*, pp. 509–515, 2010. doi: 10.1109/ICMET.2010.5598411.
- Sandler, M., Howard, A., Zhu, M., Zhmoginov, A., and Chen, L.-C. Mobilenetv2: Inverted residuals and linear bottlenecks, 2018. URL <https://arxiv.org/abs/1801.04381>.
- Siam, M., Gamal, M., Abdel-Razek, M., Yogamani, S., and Jagersand, M. Rtseg: Real-time semantic segmentation comparative study, 2018. URL <https://arxiv.org/abs/1803.02758>.
- Simonyan, K. and Zisserman, A. Very deep convolutional networks for large-scale image recognition, 2014. URL <https://arxiv.org/abs/1409.1556>.
- Strudel, R., Garcia, R., Laptev, I., and Schmid, C. Segmenter: Transformer for semantic segmentation, 2021. URL <https://arxiv.org/abs/2105.05633>.
- Szegedy, C., Liu, W., Jia, Y., Sermanet, P., Reed, S., Anguelov, D., Erhan, D., Vanhoucke, V., and Rabinovich, A. Going deeper with convolutions, 2014. URL <https://arxiv.org/abs/1409.4842>.
- Tolstikhin, I., Houlsby, N., Kolesnikov, A., Beyer, L., Zhai, X., Unterthiner, T., Yung, J., Steiner, A., Keysers, D., Uszkoreit, J., Lucic, M., and Dosovitskiy, A. Mlp-mixer: An all-mlp architecture for vision, 2021.
- Touvron, H., Cord, M., Douze, M., Massa, F., Sablayrolles, A., and Jégou, H. Training data-efficient image transformers: distillation through attention, 2020. URL <https://arxiv.org/abs/2012.12877>.
- Trockman, A. and Kolter, J. Z. Patches are all you need?, 2022. URL <https://openreview.net/forum?id=TVHS5Y4dNvM>.
- van Rijthoven, M., Balkenhol, M., Siliņa, K., van der Laak, J., and Ciompi, F. Hooknet: Multi-resolution convolutional neural networks for semantic segmentation in histopathology whole-slide images. *Medical Image Analysis*, 68:101890, 2021. ISSN 1361-8415. doi: <https://doi.org/10.1016/j.media.2020.101890>. URL <https://www.sciencedirect.com/science/article/pii/S1361841520302541>.
- Wang, H., Zhu, Y., Green, B., Adam, H., Yuille, A., and Chen, L.-C. Axial-deeplab: Stand-alone axial-attention for panoptic segmentation, 2020a. URL <https://arxiv.org/abs/2003.07853>.
- Wang, Q., Xie, J., Zuo, W., Zhang, L., and Li, P. Deep CNNs meet global covariance pooling: Better representation and

- generalization. *IEEE Transactions on Pattern Analysis and Machine Intelligence*, pp. 1–1, 2020b. doi: 10.1109/tpami.2020.2974833. URL <https://doi.org/10.11092Ftpami.2020.2974833>.
- Wightman, R. Pytorch image models. <https://github.com/rwightman/pytorch-image-models>, 2019.
- Williams, T. and Li, R. Wavelet pooling for convolutional neural networks. In *International Conference on Learning Representations*, 2018. URL <https://openreview.net/forum?id=rkhlb81CZ>.
- Wu, C. W. Prodsumnet: reducing model parameters in deep neural networks via product-of-sums matrix decompositions, 2018. URL <https://arxiv.org/abs/1809.02209>.
- Wu, H., Xiao, B., Codella, N., Liu, M., Dai, X., Yuan, L., and Zhang, L. Cvt: Introducing convolutions to vision transformers, 2021.
- Xiao, H., Rasul, K., and Vollgraf, R. Fashion-mnist: a novel image dataset for benchmarking machine learning algorithms. *CoRR*, abs/1708.07747, 2017. URL <http://arxiv.org/abs/1708.07747>.
- Xie, E., Wang, W., Yu, Z., Anandkumar, A., Alvarez, J. M., and Luo, P. Segformer: Simple and efficient design for semantic segmentation with transformers, 2021. URL <https://arxiv.org/abs/2105.15203>.
- Yu, W., Luo, M., Zhou, P., Si, C., Zhou, Y., Wang, X., Feng, J., and Yan, S. Metaformer is actually what you need for vision, 2021. URL <https://arxiv.org/abs/2111.11418>.
- Yuan, L., Chen, Y., Wang, T., Yu, W., Shi, Y., Jiang, Z., Tay, F. E., Feng, J., and Yan, S. Tokens-to-token vit: Training vision transformers from scratch on imagenet, 2021. URL <https://arxiv.org/abs/2101.11986>.
- Yun, S., Han, D., Oh, S. J., Chun, S., Choe, J., and Yoo, Y. Cutmix: Regularization strategy to train strong classifiers with localizable features. In *Proceedings of the IEEE/CVF International Conference on Computer Vision (ICCV)*, October 2019.
- Zhang, H., Cisse, M., Dauphin, Y. N., and Lopez-Paz, D. mixup: Beyond empirical risk minimization, 2017.
- Zhang, J., He, T., Sra, S., and Jadbabaie, A. Why gradient clipping accelerates training: A theoretical justification for adaptivity, 2020.
- Zhao, H., Jia, J., and Koltun, V. Exploring self-attention for image recognition, 2020. URL <https://arxiv.org/abs/2004.13621>.
- Zhong, Z., Zheng, L., Kang, G., Li, S., and Yang, Y. Random erasing data augmentation, 2017.
- Zhou, B., Lapedriza, A., Khosla, A., Oliva, A., and Torralba, A. Places: A 10 million image database for scene recognition. *IEEE Transactions on Pattern Analysis and Machine Intelligence*, 2017.

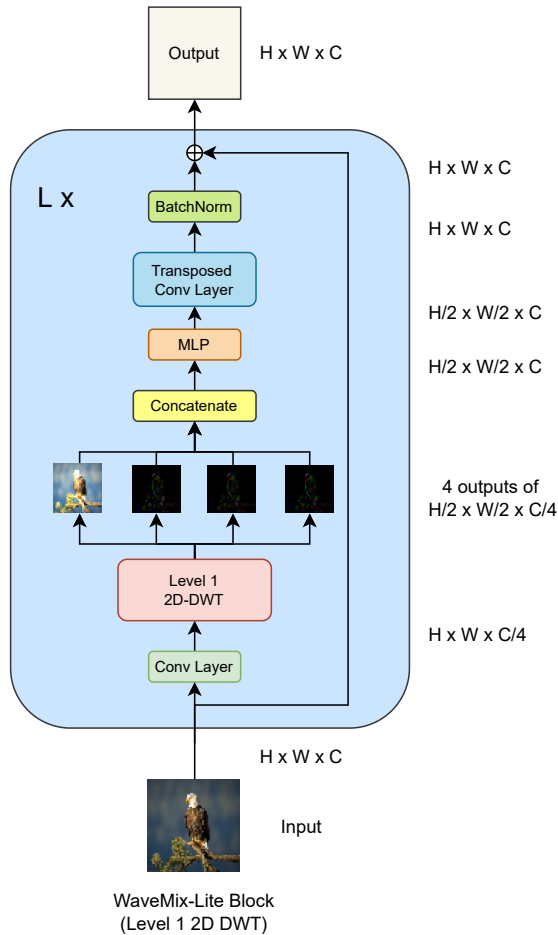


Figure 2. Details of the WaveMix-Lite block. WaveMix-Lite uses only a single level 2D-DWT

A. Feedforward Dimension and MLP Multiplication Factor

The feedforward dimension (ff) is the dimension of the embeddings of output from the MLP layer before it is passed to the deconvolution layer. The deconvolution layer then changes the embedding dimension back to the value set in the model name. Unless otherwise mentioned, the value of feedforward dimension is set by default as the embedding dimension specified in the model name. Using a value higher than embedding dimension as ff dimension increases the number of parameters of the model and GPU consumption. Feedforward dimension is different from the MLP multiplication factor (mul) which describes the increase in embedding dimension within the MLP layer (the first 1×1 convolution increases it by a factor and the second 1×1 convolution decreases it after it passes through the GELU activation). For example, MLP multiplication factor of 2 in a WaveMix-128 will use the first 1×1 convolutional layer inside MLP to increase the embedding dimension from 128

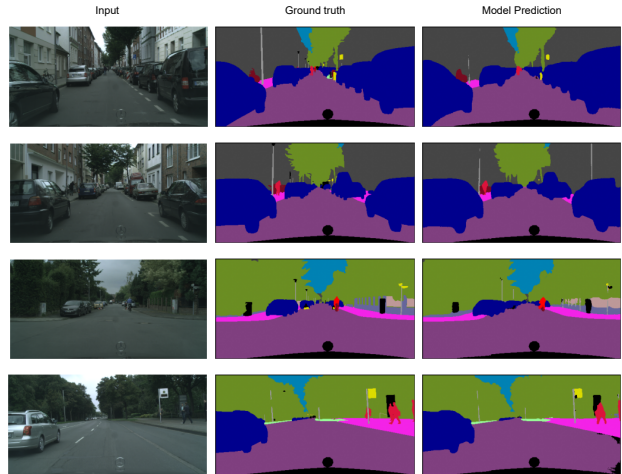


Figure 3. Qualitative results of semantic segmentation on Cityscapes dataset by WaveMix.

to 256. After the GELU activation, the second 1×1 convolutional layer inside MLP will decrease the embedding dimension back to 128. If we specify the ff dimension to be different from one provided in model name, then the second 1×1 convolutional layer inside MLP will change it to the ff dimension as specified. Unless otherwise mentioned, a MLP multiplication factor of 2 was used in all the models.

B. Semantic Segmentation

B.1. Detailed Results

The original input image resolution of 1024×2048 could not be used in most of our experiments due to resource constraints. Two strided convolutional layers were provided to reduce the input to 128×256 or 256×512 before it reaches the WaveMix layers. The 1024×2048 input size was used in 80 GB A100 GPU, 512×1024 input size was used in 40 GB A100 GPU and 256×512 input size was used for 16 GB V100 GPU. Table 6 shows the detailed results of our experiments in Cityscapes dataset. Few examples of qualitative results are provided in Figure 3.

B.1.1. ABLATION STUDIES

Influence of input image size. From Table 6 we can see that for the same model size, larger input image resolution gave better results. The results for 512×1024 input was 6-8% better than the corresponding results obtained while using input size of 256×512 . Results for input size of 1024×2048 was 2% better than 512×1024 input size.

Influence of number of layers. The number of layers that could be tested were limited due to the GPU constraints as well as the batch size requirements. We observed an

Table 6. Results for semantic segmentation using WaveMix models on Cityscapes validation dataset at different image resolutions in V100 and A100 GPUs.

ARCHITECTURE	mIOU \uparrow	# PARAM. \downarrow	MAX BATCH SIZE FOR 16 GB \uparrow	INFERENCE THROUGHPUT (FPS) \uparrow
IMAGE RESOLUTION 256×512 ON 16 GB V100 GPU				
WAVEMIX-LITE-128/8	63.33	2.9 M	55	18
WAVEMIX-LITE-128/20 (MUL 3)	67.76	7.5 M	32	17
WAVEMIX-LITE-160/12	65.08	6.6 M	45	18
WAVEMIX-LITE-192/12	65.92	9.5 M	40	19
WAVEMIX-LITE-224/12	66.67	12.9 M	32	18
WAVEMIX-LITE-256/7 (FF 160)	65.30	7.2 M	45	18
WAVEMIX-LITE-256/7 (FF 160, MUL 3)	64.34	7.9 M	40	19
WAVEMIX-LITE-256/7 (FF 192, MUL 3)	65.27	8.9 M	30	17
WAVEMIX-LITE-256/12 (FF 160)	67.11	11.5 M	30	18
WAVEMIX-LITE-256/12 (FF 192)	65.46	13.3 M	25	17
WAVEMIX-LITE-256/12 (FF 224)	66.75	15.0 M	30	18
WAVEMIX-LITE-256/12	67.46	16.9 M	25	12
WAVEMIX-LITE-256/12 (FF 1024, MUL 3)	62.39	63.2 M	22	17
WAVEMIX-LITE-256/16 (FF 272, MUL 3)	67.46	25.5 M	20	17
WAVEMIX-LITE-256/16 (FF 512, MUL 3)	71.75	44.2 M	18	18
WAVEMIX-LITE-256/16 (FF 512, MUL 4)	67.17	47.3 M	18	18
WAVEMIX-LITE-256/16 (FF 1024, MUL 3)	69.94	84 M	18	17
WAVEMIX-LITE-256/18 (FF 512, MUL 3)	65.16	49.6 M	16	17
WAVEMIX-LITE-256/20 (MUL 3)	67.65	30.1 M	16	18
WAVEMIX-LITE-256/20 (FF 512, MUL 3)	67.80	55.0 M	16	17
WAVEMIX-LITE-272/16	67.48	25.0 M	22	17
WAVEMIX-LITE-288/16	67.90	28.0 M	20	17
WAVEMIX-LITE-304/16	67.76	31.2 M	18	18
WAVEMIX-LITE-320/16 (FF 512, MUL 3)	67.94	56.5 M	15	16
WAVEMIX-LITE-512/12 (FF 1024, MUL 3)	65.09	133.2 M	11	17
IMAGE RESOLUTION 512×1024 ON 40 GB A100 GPU				
WAVEMIX-LITE-128/8	67.55	2.9 M	32	16
WAVEMIX-LITE-256/7	70.43	10.2 M	18	16
WAVEMIX-LITE-256/14	73.86	19.5 M	15	16
WAVEMIX-LITE-256/16	76.79	22.2 M	13	16
WAVEMIX-LITE-256/17	74.26	23.5 M	12	16
WAVEMIX-LITE-256/18	74.67	24.9 M	12	16
WAVEMIX-LITE-272/16	73.21	25.1 M	12	16
WAVEMIX-LITE-288/16	73.06	28.1 M	11	16
IMAGE RESOLUTION 1024×2048 ON 80 GB A100 GPU				
WAVEMIX-LITE-256/16	75.32	22.3 M	1	9
WAVEMIX-256/16 (LEVEL 2)	75.92	35.9 M	1	8
WAVEMIX-256/16 (LEVEL 3)	76.54	49.6 M	1	7
WAVEMIX-256/15 (LEVEL 4)	77.18	59.4 M	1	7
WAVEMIX-256/16 (4 LEVEL)	78.64	63.2 M	1	7
WAVEMIX-256/17 (LEVEL 4)	77.68	67.1 M	1	6

Table 7. Performance of WaveMix models on different datasets

DATASET	MODEL	ACC. (%)
SVHN	WAVEMIX-LITE-144/15	98.73
PLACES-365	WAVEMIX-240/12 (4 LEVEL)	56.45
INAT-2021	WAVEMIX-256/16 (2 LEVEL)	61.75

increase in mIoU as the number of layers increases, then it peaks at around 16 layers for various input sizes and then gradually decreases for each additional layer.

Influence of embedding dimension. We varied the embedding dimension from 128 to 512 in the V100 GPU. The number of layers were adjusted to keep the model fit in the single GPU. For the A100 GPU, it was varied from 128 to 288. Variation of embedding dimension showed a behaviour similar to that shown by increasing the number of layers where mIoU first increases with increase in embedding dimension, then peaks at around 256, and then starts to decrease for both the input image sizes.

Influence of the MLP multiplication factor. Table 6 shows that increasing the multiplication factor (mul) does not increase the parameter count significantly. It can be used to vary the parameter count slightly for a marginal increase the performance. Increasing the MLP multiplication factor beyond 3 showed slight deterioration in performance with input images of size 256×512 .

Influence of multiple levels of Wavelet transforms Table 6 shows that using multi-level 2D-DWT provides better results than just using a single level (WaveMix-Lite). The best results were obtained when using 4 levels of 2D-DWT for an input size of 1024×2048 .

C. Image Classification

C.1. Results on Smaller Resolution Image Datasets

We observe from Table 8 that deeper WaveMix models perform better and this suggests that even further scale-up of WaveMix in multi-GPU setting could be possible. We see from Table 9 that shallow WaveMix models are competitive in performance to deeper ResNets and MobileNets, and they are approximately 2x faster in training 4x faster in inference. Even deeper WaveMix models provide faster inference and better performance compared to the other models. ConvMixers are parameter-efficient and provide high accuracy, but they need much higher GPU RAM compared to WaveMix.

In Table 10 we see that on CIFAR and TinyImageNet datasets, WaveMix-Lite performs much better than the other models, giving accuracy higher than ResNets and MobileNets with 4 to 10 times fewer parameters and less

Table 8. Image classification results on ImageNet-1K dataset (224×224) without augmentations by WaveMix (arrows in column headers show desired directions). Patch size of 5 is used for WaveMix-Lite models and 4 is used for other WaveMix models. Training was not done using Timm training script.

MODELS	TOP-1 ACCU. (%) \uparrow	# PARAM. \downarrow
WAVEMIX-LITE-192/12	64.05	10.7 M
WAVEMIX-LITE-256/16	65.88	23.4 M
WAVEMIX-224/12 (2 LEVEL)	65.90	22.6 M
WAVEMIX-240/12 (2 LEVEL)	66.44	25.8 M
WAVEMIX-208/12 (3 LEVEL)	68.24	25.7 M
WAVEMIX-192/16 (3 LEVEL)	68.85	28.9 M
WAVEMIX-224/12 (3 LEVEL)	69.56	29.4 M
WAVEMIX-240/12 (3 LEVEL)	70.02	33.8 M

GPU consumption. GPU consumption of WaveMix-Lite is sometimes 50 times lower for similar performance when compared to transformer models.

C.2. Augmentations and Learning Rate Tuning

The previously reported results for the other architectures include the effect of various well-intentioned incremental training methods (tips and tricks) like Timm training script (Wightman, 2019), including RandAugment (Cubuk et al., 2019), mixup (Zhang et al., 2017), CutMix (Yun et al., 2019), random erasing (Zhong et al., 2017), gradient norm clipping (Zhang et al., 2020), learning rate warmup (Gotmare et al., 2019) and cooldown. These additional methods improve the results of the core architectures trained using simple methods by a few percentage points each. For example, Mixup, Cutmix, Random Erasing, RandAugment, Random Scaling and Gradient Norm Clipping improved accuracy of ConvMixer by 9.55 percentage points in image classification (Trockman & Kolter, 2022). However, experimenting with these additional training methods requires extensive hyperparameter tuning. On the other hand, by excluding these methods, we were able to compare the contribution of the base architectures in a uniform manner. The accuracy obtained in our experiments for the other architectures are thus lower than the previously reported numbers, but the results are still within the expected range when such training methods are not used. We noticed an improvement of 5.58 percentage points (64.45% to 69.93%) just by using default parameters in the Timm training script (Wightman, 2019) for ImageNet-1K classification using WaveMix-Lite-256/16. WaveMix should be able to outperform the reported results of other models when we do proper hyper-parameter tuning in Timm library.

WaveMix: A Resource-efficient Neural Network for Image Analysis

Table 9. Image classification on ImageNet-1K dataset (224×224) without augmentations shows improved accuracy as well as throughput due to decreased parameter count and GPU RAM consumption by WaveMix (arrows in column headers show desired directions).

ARCHITECTURE	TOP-1 ACCU.	# PARAM. ↓	GPU RAM FOR	THROUGHPUT (IM/S)	
	(%) ↑		BATCH SIZE 64 ↓	TRAIN ↑	TEST ↑
RESNET-18	55.12	11.7 M	2.7 GB	450	439
RESNET-34	57.02	21.8 M	3.1 GB	414	410
RESNET-50	61.76	25.6 M	6.2 GB	638	617
RESNET-101	64.60	44.5 M	9.6 GB	487	725
RESNET-152	65.86	60.2 M	12.7 GB	344	758
MOBILENETV3-SMALL	51.57	2.5 M	1.4 GB	255	229
MOBILENETV3-LARGE	58.89	5.5 M	3.5 GB	492	481
<hr/>					
ViT-B-16	39.53	86.6 M	10.0 GB	140	420
ViT-B-32	30.11	88.2 M	2.2 GB	1,595	1,613
CPV-256/5x4	63.02	6.7 M	12.9 GB	364	728
<hr/>					
CONVMIXER-512/12	60.24	4.2 M	10.8 GB	292	735
CONVMIXER-512/16	62.24	5.4 M	14.1 GB	220	725
CONVMIXER-1024/12	64.13	14.6 M	23.6 GB	251	667
<hr/>					
WAVEMIX-LITE-128/8	54.12	3.9 M	4.5 GB	1,242	1,724
WAVEMIX-224/12 (2 LEVEL)	65.90	22.6 M	9.8 GB	385	1,250
WAVEMIX-240/12 (3 LEVEL)	70.02	33.8 M	15.6 GB	205	610

Table 10. Results for image classification on small datasets (32x32, 64x64) show improved accuracy as well as decreased parameter count and GPU RAM consumption by WaveMix-Lite. No augmentations were used.

MODEL	#PARAM. ↓	GPU RAM FOR BATCH SIZE 64 ↓	ACCURACY (%) ↑		
			CIFAR-10	CIFAR-100	TINYIMNET
RESNET-18 (HASSANI ET AL., 2021)	11.20 M	1.2 GB	90.27	63.41	48.11
RESNET-34 (HASSANI ET AL., 2021)	21.30 M	1.4 GB	90.51	64.52	45.60
RESNET-50 (HASSANI ET AL., 2021)	25.20 M	3.3 GB	90.60	61.68	48.77
MOBILENETV2 (HASSANI ET AL., 2021)	8.72 M	-	91.02	67.44	-
ViT-128/4x4	0.53 M	13.8 GB	56.81	30.25	26.43
ViT-384/12x6 (HASSANI ET AL., 2021)	85.60 M	-	76.42	46.61	-
ViT-LITE-256/6x4 (HASSANI ET AL., 2021)	3.19 M	-	90.94	69.20	-
HYBRIDViN-128/4x4	0.62 M	4.8 GB	75.26	51.44	34.05
CCT-128/4x4	0.91 M	15.8 GB	82.23	57.09	39.05
CvT-128/4x4	1.12 M	15.4 GB	79.93	48.29	40.69
MLP-MIXER-512/8	2.41 M	1.0 GB	72.22	44.23	26.83
<hr/>					
WAVEMIX-LITE-16/7	0.04 M	0.1 GB	64.98	23.03	19.15
WAVEMIX-LITE-32/7	0.15 M	0.3 GB	84.67	46.89	34.34
WAVEMIX-LITE-64/7	0.60 M	0.6 GB	87.81	62.72	46.31
WAVEMIX-LITE-128/7	2.42 M	1.1 GB	91.08	68.40	52.03
WAVEMIX-LITE-144/7	3.01 M	1.2 GB	92.97	68.86	52.38
WAVEMIX-LITE-160/13	6.90 M	9.4 GB	-	-	54.76
WAVEMIX-LITE-256/7	9.62 M	2.3 GB	90.72	70.20	51.37

Table 11. Comparison of Top-1 Accuracy of WaveMix models using different initial convolution layers on ImageNet-1k dataset. Patch size of 4 is used in patchify layer

MODEL	STRIDED CONVOLUTIONS	PATCHIFYING LAYER
WAVEMIX-LITE-224/20	62.79	67.91
WAVEMIX-240/12 (2 LEVEL)	64.75	66.44
WAVEMIX-240/12 (3 LEVEL)	67.97	70.02

Table 12. State-of-the-art (SOTA) models for the 5 EMNIST Datasets.

DATASET	MODEL	ACC.(%)
BY_CLASS	WAVEMIX-LITE-128/7	88.43
BALANCED	WAVEMIX-LITE-128/7	91.06
LETTERS	WAVEMIX-LITE-112/16	95.96
DIGITS	WAVEMIX-LITE-112/16	99.82
BY_MERGE	WAVEMIX-LITE-128/16	91.80

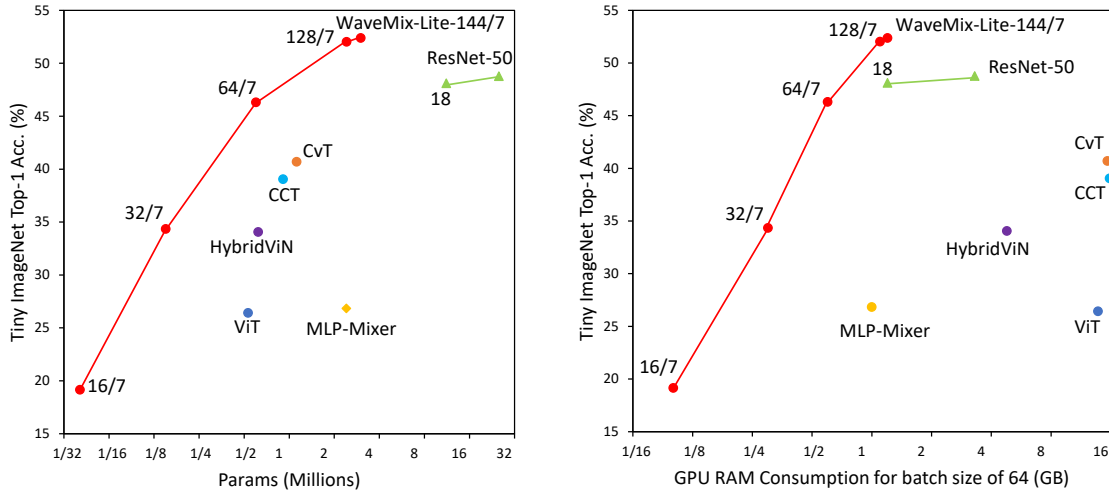


Figure 4. Accuracy scales more efficiently with parameters and GPU RAM for WaveMix-Lite compared to transformers and ResNets

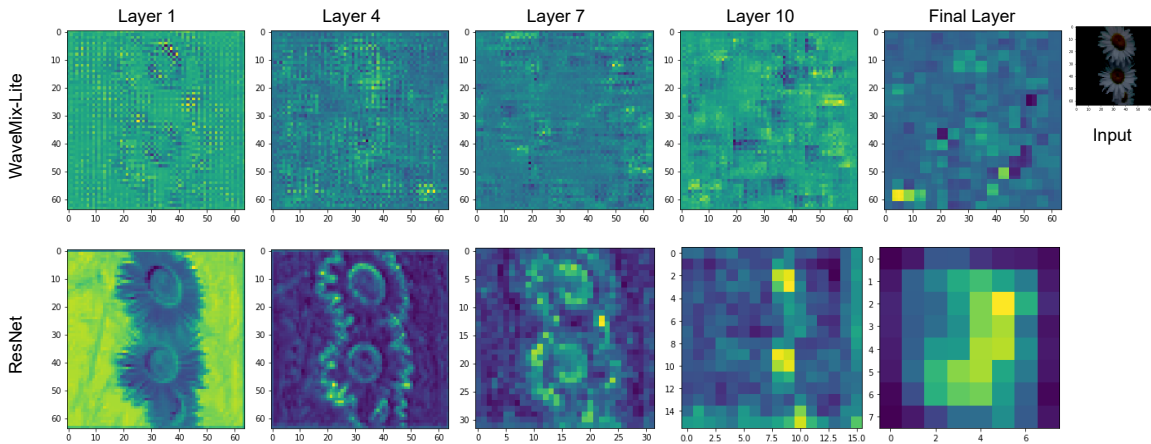


Figure 5. Visualisation of outputs after each layer shows that the image representation is different in WaveMix-Lite and ResNet.

Table 13. Comparison of performance for image classification on CIFAR-10 dataset by WaveMix-Lite-256/7 using various different Wavelets show that Haar Wavelet is better.

Wavelet	Top-1 Acc. (%)	Time for one epoch (s)
Haar (db1)	91.15	25
Daubechies (db2)	90.72	44
Daubechies (db3)	89.14	68
Daubechies (db4)	88.00	104
Daubechies (db5)	86.88	148
Biorthogonal (bior1.3)	90.50	67
Biorthogonal (bior1.5)	89.61	157
Reverse Biorthogonal (rbio 1.3)	90.14	67
Coiflet (coif1)	89.98	67
Coiflet (coif2)	85.68	233
Symlet (sym2)	90.24	44
Symlet (sym3)	88.87	63

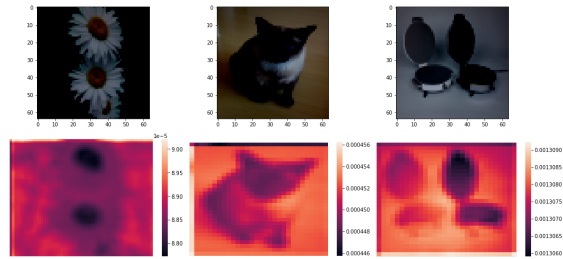


Figure 6. The results of occlusion analysis to find the significance of each pixel in the output decision shows that WaveMix identifies all the right pixels in an image for making the classification decision. The darker pixels in the image contribute more to the decision than lighter ones. The numbers show the probability of class output when the pixel is occluded.

Table 14. Variation of performance and resource consumption of WaveMix-Lite-144/7 on classification of CIFAR-10 dataset using different levels of 2D-DWT separately.

LEVEL OF 2D-DWT	ACCU. (%)	# PARAMS	GPU FOR BATCH SIZE OF 1024
1	91.61	3 M	19.6 GB
2	87.39	5.9 M	14.2 GB
3	78.07	15.2 M	13.7 GB
4	65.40	47.7 M	13.2 GB

C.3. Ablation Studies

Influence of initial convolutional layers. We experimented with two types of convolutional layers in the initial convolutional layer to downscale the image size for large resolution datasets. Strided convolutions with stride of 2 reduced the resolution by half in each layer. In patchifying convolutional layer, we used 2 layers of normal convolutions followed by a patchifying convolutional layer (stride and kernel size set to same value), a GELU non-linearity and a batch normalisation layer. We see from Table 11 that using patchifying convolutions perform better than strided convolutions for WaveMix models.

Influence of levels of 2D-DWT. Table 14 shows the variation of performance and resource consumption for each level of 2D-DWT. Level-1 2D-DWT reduced image resolution by half, reducing the computational cost and GPU consumption compared to convolutional layers. Using higher levels of 2D-DWT could further reduce the image resolution to one-fourth, one-eighth and so on which can further reduce the computational costs. But the deconvolution layer used to resize the output back to input size will need a lot more parameters. This will consume more resources in terms of GPU and time. Each increment in the level of 2D-DWT results in doubling of the number of parameters, but provides only a very small reduction in GPU consumption, especially when we go to higher levels of 2D-DWT. In each of the higher level decompositions, when the approximation and detail coefficients are concatenated as a tensor, the noise intensity in the detail coefficients would be stronger than that of useful details (object edge, texture, or contour, etc.) which could be the cause of degradation in the performance. When we use multiple levels of 2D-DWT together, we observe a gain in performance as we add more levels as shown in Table 8 for high resolution images. This improvement in performance was not observed for low resolution images when we used more than 1 level of 2D-DWT (WaveMix-Lite).

Influence of number of layers. The performance of WaveMix models generally improve as the number of layer increases. The behaviour observed in smaller datasets show

that the accuracy increases with increase in number of layers, peaks at a particular value and then do not show any increase for any further addition of layers. In experiments with ImageNet-1k dataset, we observed that while using higher levels of 2D-DWT, the number of layers needed is much lower for reaching the best performance when compared to WaveMix-Lite. Therefore, WaveMix with multilevel 2D-DWT are shallower than WaveMix-Lite.

Influence of the Embedding Dimension. Our experiments showed that increasing the embedding dimension of a model usually improved the model performance, but the resource-utilization also increased significantly. Doubling the embedding dimension of model from 128 to 256 results in an increase of parameter count by more than three times and doubles the GPU RAM consumption.